

Period-doubling Instability of Bose-Einstein Condensates Induced in Periodically Translated Optical Lattices

Nathan Gemelke¹, Edina Sarajlic¹, Yannick Bidel¹, Seokchan Hong² and Steven Chu³

¹Department of Physics, Stanford University, Stanford, CA 94305

²Department of Applied Physics, Stanford University, Stanford, CA, 94305

³Directorate, Lawrence Berkeley National Lab, Berkeley, CA 94720

(Dated: March 23, 2024)

We observe the formation of momentum distributions indicative of spatial period-doubling of superfluid Bose-Einstein condensates in periodically translated optical lattices. The effect is attributed to dynamical instability of the condensate wavefunction caused by modulation-induced coupling of ground and excited bands.

PACS numbers: 03.75.Kk, 03.75.Lm, 32.80.Lg, 05.45.Yv

Atomic Bose-Einstein condensates in optical lattice potentials have been a focus of many studies in the last decade, serving as a model system for study of traditionally solid state phenomena. Interparticle interaction, in combination with the periodicity of the lattice potential, give rise to interesting nonlinear dynamics, such as gap soliton formation [1] and instabilities [2, 3]. These have been successfully described by the Gross-Pitaevskii equation (GPE), which describes the mean-field evolution of the condensate wavefunction. Stationary solutions of the GPE have been shown to include Bloch waves, as well as non-Bloch states with longer spatial periodicity [4], and have been predicted to be energetically and dynamically unstable for specific quasimomenta [4, 5]. Instability occurs when the excitation spectrum of the condensate is altered by the periodic potential and interaction in such a way as to make the macroscopic wavefunction unstable to perturbation. This has been experimentally demonstrated with condensates accelerated relative to the lattice [2, 3].

We report here on the observation of a period-doubling dynamical instability introduced by periodically translating (shaking), the optical lattice potential. This perturbation couples vibrational levels in the lattice and creates an effective band structure through interference of tunneling amplitudes for atoms in superposed vibrational states. The onset of instability is detected by directly observing the sudden growth of narrow momentum components of the condensate wavefunction at half the lattice recoil momentum, corresponding to perturbation modes which modulate the condensate wavefunction with a period of two lattice spacings. The critical onset threshold with shaking amplitude and frequency is measured and compared to the behavior expected from calculated band structure and numeric evolution of the GPE.

To observe these effects, samples of 5×10^4 Bose-condensed ^{87}Rb atoms were prepared in the $F = 2; m_F = 2$ hyperfine state with no observable thermal component by evaporative cooling in a triaxial TOP trap [6, 7]. After evaporation, the magnetic trap frequencies were relaxed to $(\hbar\omega_{\text{qp}}; \hbar\omega_{\text{np}}; \hbar\omega_z) = 2(55; 32; 28)\text{Hz}$, and the condensate was adiabatically loaded into a set of 1, 2 or 3 orthogonal standing waves derived from a

10W, 1.064 μm Nd:YAG laser injected by a stable seed laser (Lightwave NPRO model 125). Two standing waves made a 45° angle with the vertical, while the third was horizontal; each standing wave was formed by one retroreflected beam focused to 100 μm at the location of the condensate, and separated in frequency from the other standing waves by 80 MHz. All beam intensities were actively stabilized to $< 1\%$ RMS over 2s. A diabatic loading was achieved by linearly ramping the standing wave intensities over 400 ms. To enable dynamical translation of the lattice potential, an electrooptic phase modulator was placed in the retroreflection path of each standing wave. In this work we used sinusoidal phase modulation $\phi(t) = \phi_0 \cos(\omega_D t)$, which translated the lattice potential in the lab frame according to $V_{\text{latt}}(\mathbf{x} - \mathbf{x}_0(t))$, where $\mathbf{x}_0(t) = \mathbf{x}_0 \cos(\omega_D t)$ is the modulation amplitude and ω_D its frequency. We calibrated the lattice by locating the heating resonance corresponding to phase modulation at the lattice vibrational frequency ω_{vib} , where $\hbar\omega_{\text{vib}}$ is the energy difference between the lowest two band centers. When multiple standing waves were used, their intensities were adjusted to equalize the vibration frequencies along all directions.

After loading and interrogating condensates in the optical lattice, the magnetic trap and lattice were switched off in 200 μs , and the atoms were absorptively imaged [8] after a 30 ms time-of-flight. The condensate momentum distribution was inferred from the matter wave interference patterns of the released atoms. Without modulation, we observed interference peaks at momenta of $n\hbar k$, where n is an integer, k is the inverse lattice vector, indicating phase-coherent localization in the lattice potential wells. Here, $\hbar k = 2\hbar/a = 2\hbar k_{\text{light}}$, where a is the lattice spacing and k_{light} is the wavevector of the light forming the optical lattice. The relative peak heights were determined by the on-site wavefunction of the condensate, whose center of mass oscillated (Fig. 1b) when the lattice was shaken near resonance.

Modulating at a frequency below resonance in a one-dimensional lattice resulted in the growth of narrow peaks at momenta of $\sim \hbar k = 2\hbar k_{\text{light}}$ (Fig. 1a), which also oscillated in phase with the drive (Fig. 1b). The presence of peaks spaced by $\sim \hbar k = 2\hbar k_{\text{light}}$ indicates periodicity of the con-

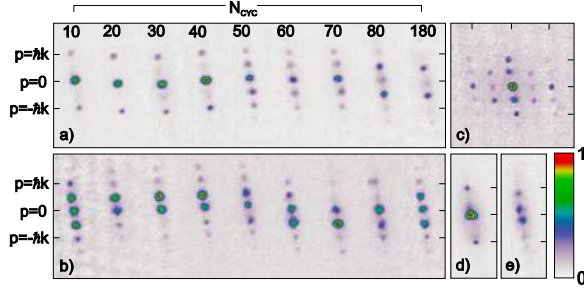


FIG. 1: Absorption images of the atomic interference following lattice modulation and time-of-flight expansion. (a) Atoms are released at the turning-point of the lattice translation, after a variable number of modulation cycles, N_{cyc} . For short modulation times, peaks occur only at $p = 0$ and $p = \pm k$. For longer times, peaks develop at $p = \pm k/2$. (b) Release occurs within the 76th cycle, spaced by $\pi/4$ in phase; the center of mass oscillates nearly in phase with the applied drive. (c) Simultaneous doubling in a 2D lattice achieved by applying the same modulation as in (a,b) to two orthogonal standing waves. (d) The effect of modulation above resonance in a 1D lattice; for small amplitudes, the $p = 0$ peak develops a shoulder. At larger amplitudes, (e) broad peaks are apparent between $p = 0$ and $p = \pm k$. For visibility, (c) shows atomic absorption; (a,b,d,e) show atomic column densities. Modulation and lattice parameters were (a,b,c) $\nu_{\text{vib}} = 2 \times 10.4 \text{ kHz}$, $x_0 = 0.04 \mu\text{m}$, $\Delta_D = 2 \times 7.6 \text{ kHz}$; (d) $\nu_{\text{vib}} = 2 \times 11.0 \text{ kHz}$, $x_0 = 0.035 \mu\text{m}$, $\Delta_D = 2 \times 12.5 \text{ kHz}$; (e) $\nu_{\text{vib}} = 2 \times 11.0 \text{ kHz}$, $x_0 = 0.037 \mu\text{m}$, $\Delta_D = 2 \times 12.5 \text{ kHz}$.

densate wavefunction on a lengthscale of twice the lattice spacing. These peaks became visible only beyond a critical frequency-dependent drive amplitude and following a sufficiently long modulation time. For a typical lattice depth of $9E_{\text{rec}}$, where $E_{\text{rec}} = \frac{\hbar^2 k^2}{8m}$, onset occurred after 5 ms of modulation with amplitude greater than $0.01a$ at a detuning of $\Delta_D = \nu_{\text{vib}} = 2 \times 2 \text{ kHz}$. The amplitude for critical onset of this momentum class decreased with decreased detuning from resonance (Fig. 2). Following onset, peaks were discernable under drive for 800 cycles (100 ms), after which they were obscured by a loss of contrast in the interference pattern. We have found similar behavior at negative detunings for lattice depths from 3.9 to $19.5E_{\text{rec}}$.

We have investigated the dependence of the critical drive parameters on the external trapping geometry by varying the envelope trapping frequencies by 30%. This caused no shift in the onset amplitude at a fixed detuning to 10%. We have also observed period-doubling in two-dimensional lattices of the same depth with one or both (Fig. 1c) axes shaken. Though a decreased contrast in the interference patterns was observed, there was no measurable shift in the period-doubling onset amplitude at a fixed detuning. In three-dimensional lattices, loss of contrast precluded observation of coherent populations at $p_j = \pm k/2$.

This sudden transition to non-zero momentum states is made possible by the effect of coupling the ground

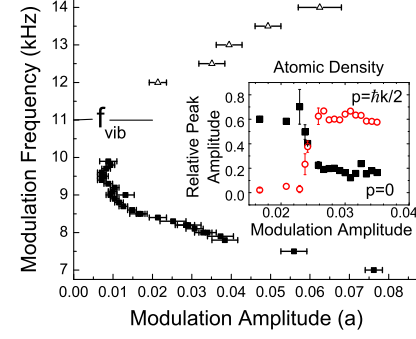


FIG. 2: Critical drive strengths and detunings. For $\Delta_D < 0$, the period-doubling onset amplitude decreases near resonance. For $\Delta_D > 0$, the $p = 0$ peak develops a shoulder, and the $p = \pm k/2$ classes are populated diffusely; these onsets are marked by open triangles. The inset shows relative peak atomic density at $p_j = 0; \pm k/2$ extracted from absorption images as a function of drive amplitude. Modulation pulse lengths for this data were 10 ms.

and first excited bands via near-resonant translation of the lattice potential. However, this perturbation acts equally on each lattice site and cannot itself induce modulations of the wavefunction at twice the lattice spacing. Interparticle interaction, however, does allow for spontaneous breaking of this discrete translational symmetry, and permits coupling between zero and non-zero quasimomentum states. Accordingly, we consider as candidate mechanisms for this effect those involving the combined influence of interaction and lattice modulation.

In the absence of modulation, Bloch states close to the first band center are stable against decay into other modes [5]. Since the second band displays a comparatively large, inverted tunneling rate, small modulation-induced admixtures of this state will dramatically alter the form of the single-particle dispersion, and the stability of Bloch waves must be reconsidered. For the case of far off-resonant modulation, band-mixing effects have previously been described [9] and observed [10] for thermal atoms. This effect becomes more apparent if we consider the two lowest bands in a 'dressed' basis set similar to that in [9]. Here, each basis state is a time-dependent superposition of delocalized ground and excited states with the same quasimomentum, chosen to make the single-particle Hamiltonian time-independent (in a rotating wave approximation) and diagonal.

The resulting band structure (Fig. 3) can be used to examine stability of stationary states in the presence of interaction. As modulation amplitude is increased, the lower dressed band is attenuated by its growing admixture of the bare excited band, and eventually inverts its curvature at the band center. In analogy with results for lowest band Bloch wave stability in the tight-binding limit [4, 5, 11], one might postulate the emergence of

a dynamic instability of the $q=0$ state near the drive strength sufficient to invert the curvature of the lower dressed band. This criterion is equivalent to developing negative effective mass, and may be considered analogous to the case of attractive interaction with positive effective mass. This prediction shows a qualitative agreement with the experimental data (Fig. 4) for $\delta < 0$.

To test this hypothesis, we performed linear stability analysis of the lattice-periodicity Bloch states for the lower dressed band in the tight-binding limit of the GPE, following methods in [4, 5]. Adding a small perturbation of well-defined momentum to Bloch waves in this band, we looked for a parameter region where the spectrum of excitations includes imaginary values, signaling exponential growth or decay of perturbations to the wavefunction. For negative detunings, one finds that zero momentum Bloch states first become dynamically unstable when the modulation amplitude becomes sufficient to make the energy at the band edge equal to that at the band center [12]. Neglecting higher-order tunneling contributions, this condition is equivalent to demanding that the probability for an atom to hop to nearest neighbor sites is zero, while the hopping rate to next-nearest neighbor sites may remain nonzero. Close to onset, exponential growth occurs only for perturbations with momentum close to $\sim k=2$, consistent with experimental observations of sharp peaks at that momentum. The predicted threshold amplitudes for instability are smaller than those necessary to invert the effective mass, and show a better quantitative agreement with experimental data (Fig. 4) at large negative detunings. This interpretation fails for small detunings, where the interaction energy exceeds the dressed band gap and introduces a non-negligible level mixing.

We note that the curves shown in Fig. 4 were calculated with knowledge only of the measured lattice vibration frequency, from which we calculate the unperturbed band structure, tunneling rates J for each band, and Wannier wavefunctions $\psi(x)$. Coupling between bands is modeled by converting to a frame moving with the lattice, resulting in a single particle hamiltonian $H = \frac{p^2}{2m} + V_{\text{latt}}(x) + m \ddot{x}_0(t)$ [9]. Here the effect of phase modulation is replaced by an inertial force, which gives an inter-band coupling strength $\sim m \ddot{x}_0(t) \int dx \psi_0^*(x) \psi_1(x)$. The on-site interaction energy is estimated by approximating the on-site wavefunction transverse to the lattice (r_\perp) by a Thomas-Fermi profile corresponding to measured transverse trapping frequencies and an estimated average occupation number. The interaction energy for atoms in bands i and j is then given by $U_{ij} = \frac{4\pi \hbar^2 a_s (2\pi)^{-2}}{m} \int dr_\perp \int dr_\parallel \psi_i^*(r_\perp, r_\parallel) \psi_j(r_\perp, r_\parallel) \psi_j^*(r_\perp, r_\parallel) \psi_i(r_\perp, r_\parallel)$, where $\psi(r) = \psi(r_\perp) \psi(r_\parallel)$, a_s is the s-wave scattering length, and m the atomic mass. For simplicity, we approximate the on-site interaction energy U_{ij} as independent of site and occupation number; more accurate treatments may be found in [13, 14].

To model the dynamics of the experiment, we have numerically evolved the GPE in the tight-binding limit

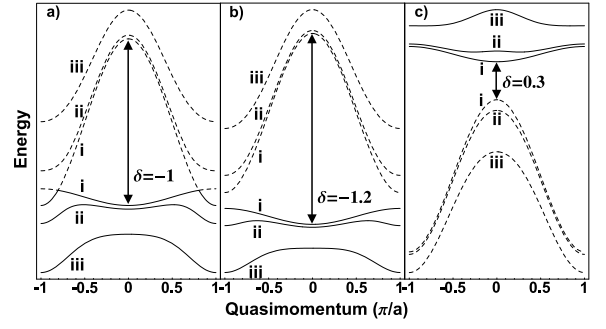


FIG. 3: Renormalized band structure for negative (a,b) and positive (c) drive detuning, as calculated by diagonalizing the single particle hamiltonian in the dressed basis, including only the two lowest bands. Solid (dashed) lines indicate the energy of the renormalized ground (excited) band. These were calculated for a lattice depth of $10.5 E_{\text{rec}}$, and inter-band coupling strengths \sim of i) 0, ii) 0.3 and iii) 0.9 E_{rec} . Detuning is labeled in units of E_{rec} .

for two coupled bands. Using the approach from [15, 16], we describe the condensate wave function with a complex site-dependent amplitude c_j for each (bare) vibrational level j , $\psi_j = \sum_j c_j \psi_j(x)$ (ψ_j is the Wannier wavefunction). We substitute ψ_j into the GPE and numerically evolve the amplitudes c_j , according to

$$i\hbar \dot{c}_j = -J(c_{j+1} + c_{j-1}) + V_j c_j + \frac{U}{2} c_j^2 + \frac{U}{4} c_j^2 + \frac{U}{2} c_j^2 + \sim \cos(k_D t) c_j, \quad (1)$$

where

$$V_j = \frac{1}{2} m \dot{x}_0(t)^2 + \sim \psi_{\text{vib}}^2 + m \ddot{x}_0(t) \psi_j \quad (2)$$

represents the external trapping potential, band energy and the intra-band effect of the inertial force. We initialize the calculation with a lower band wavefunction solved to be stationary in absence of modulation. The chemical potential is chosen to reproduce the number of atoms N in the experiment. The calculation was performed with an external potential comparable to that used in the experiment, and number of sites chosen to safely exceed the number occupied in the experiment.

The parameters for onset of the $\sim k=2$ peaks at negative drive detunings show good agreement with those observed in the experiment (Fig. 4), and agree well with the prediction for instability at the center of the lowest dressed band described above for large detuning. We have performed the same numerical evolution for an excited state with a positive tunneling amplitude; in this case, no period-doubling was observable.

To investigate the importance of the external trapping potential, we compare period-doubling onsets with and without \ddot{x}_0 . To reduce numeric artifacts stemming from the large inertial force and boundary effects, this comparison was done in the stationary frame, to first order in

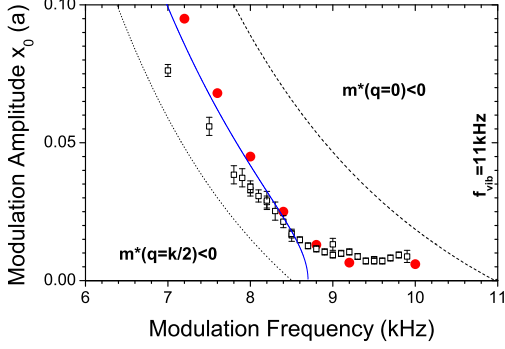


FIG. 4: Comparison of experimental and numeric data for drive parameters at onset. Boxes show experimental data points for onset under same conditions as Fig. 2. Solid line shows analytic result for equal single-particle energy at band center and edge, which occurs for zero drive amplitude when bands cross. Dashed (dotted) line shows line of infinite effective mass at band center (edge). Between dashed and dotted lines effective mass is positive both at band center and edge. Circles show onset in numeric evolution of the GPE for $J_0 = 0.024$; $J_1 = 0.28$; $U_{00} = U_{10} = (4/3)U_{11} = 2 \times 10^{-4}$ in units of E_{rec} ; $\Omega_{\text{ext}} = 2 \times 45 \text{ Hz}$ and $N = 5 \times 10^4$. Note that the numeric data is a zero-parameter comparison to experimental data generated from the measured Ω_{vib} .

the lattice displacement amplitude x_0 . Without the external potential, periodic boundary conditions were used with a site number comparable to the experiment (40). In this case, we find a small initial seed population at $p = \sim k=2$ grows rapidly once a sufficient modulation strength is applied. Without a seed population, observable peaks at $\sim k=2$ do not occur for experimentally relevant timescales. With an external trapping potential this seed population is guaranteed by the finite extent of the condensate wavefunction, and numerically results in an observable population at $p = \sim k=2$ in several ms, consistent with experimental observations. This suggests that, while the mechanism for period-doubling exists on a lattice with discrete translational symmetry, the on-

set of the period-doubling population is hastened by an external potential through its effect on the initial state.

The analysis above applies to modulation performed below resonance, where the influence of the avoided crossing in Fig. 3 is felt most strongly at the band edge. Experimentally, modulation performed at frequencies higher than the vibrational resonance first results in the appearance of a shoulder around the $p=0$ peak, followed by growth of broad peaks around $p = \sim k=2$ (Fig. 1d,e). The critical drive amplitude necessary for this behavior is higher than for the period-doubling onset at an equal detuning of opposite sign (Fig. 2). While such behavior might be expected from the band structure in curve ii of Fig. 3c, the details of its onset and dynamics are not yet fully understood.

In conclusion, we have experimentally observed a period-doubling instability of a ^{87}Rb condensate held in a shaken optical lattice potential, and determined the threshold modulation conditions necessary for the onset of this behavior. A simple physical interpretation provides qualitative agreement with the onset of the observed dynamic instability, while a numerical simulation of the effect based on the GPE is in quantitative agreement with this picture.

A new feature in this observation of dynamic instability is the controlled introduction of instability at zero quasimomentum and the ability to directly observe the growth of a well-defined unstable mode. Due to the depth and dimensionality of the lattices used, it is interesting to consider the effect of fluctuations of the long range coherence of the condensate near the onset of this instability. In the dressed-state picture, the modulation-induced attenuating of the lower band at $q=0$ further increases the already large ratio of local interaction energy to tunneling amplitude, pointing to an increasing importance of fluctuations and limited validity of a mean field description. In this light, a description beyond that of the GPE may warrant future study.

We wish to thank Christopher Pethick, Mark Kasevich, Shoucheng Zhang and Congjun Wu for helpful discussions. This work was supported in part by grants from AFOSR and the NSF.

-
- [1] B. Eiermann, T. Anker, M. Albiez, M. Taglieber, P. Treutlein, K. P. Marzlin, and M. K. Oberthaler, Phys. Rev. Lett. 92, 230401 (2004).
 - [2] F. Cataliotti, L. Fallani, F. Ferlano, C. Fort, P. Maddaloni, and M. Inguscio, New J. Phys. 5, 71 (2003).
 - [3] L. Fallani, L. De Sarlo, J. Lye, M. Modugno, R. Saers, C. Fort, and M. Inguscio, Phys. Rev. Lett. 93, 140406 (2004).
 - [4] M. Machholm, A. Nicolini, C. Pethick, and H. Smith, Phys. Rev. A 69, 043604 (2004).
 - [5] B. Wu and Q. Niu, Phys. Rev. A 64, 061603(R) (2001).
 - [6] W. Petrich, M. Anderson, J. Ensher, and E. Cornell, Phys. Rev. Lett. 74, 3352 (1995).
 - [7] J. Müller, D. Ciampini, O. Morsch, G. Semer, M. Fazzi, P. Verkerk, F. Fuso, and E. Arimondo, J. Phys. B 33, 4095 (2000).
 - [8] W. Ketterle, D. Durfee, and D. Stamper-Kurn, in Proceedings of the International School of Physics - Enrico Fermi, Inguscio et al. eds p. 67 (1998).
 - [9] R. D'ienier and Q. Niu, J. Opt. B 2, 618 (2000).
 - [10] K. Madison, M. Fischer, R. D'ienier, Q. Niu, and M. Raizen, Phys. Rev. Lett. 7, 5093 (1998).
 - [11] C. Menotti, A. Smerzi, and A. Trombettoni, New J. Phys. 5, 112 (2003).
 - [12] N. Gemelke, E. Sarajlic, Y. Bidel, S. Hong, and S. Chu, in preparation.

- [13] A .Sm erzi and A .T rom bettoni, Phys.Rev.A 68, 023613 (2003).
- [14] L.Salas nich, A .Parola, and L.Reatto, Phys.Rev.A 65, 043614 (2002).
- [15] A .T rom bettoni and A .Sm erzi, Phys.Rev.Lett.86, 2353 (2001).
- [16] G .A l m ov, P .K evrekidis, V .K onotop, and M .Salemo, Phys.Rev.E 66, 046608 (2002).